

Fabrication of Solution-Processed Perovskite Solar Cells for Low-Light Energy Harvesting Applications

Izzah Afifah Ibrahim¹, Muhammad Fakhrullah Mohamad Azmi¹, Irfan Danial Ismadi¹,
Muhammad Fadzliyam Redzuan¹, Ikhwan Syafiq Mohd Noor², Nizam Tamchek²,
Mohd Ifwat Mohd Ghazali¹, Wan Haliza Abd Majid³ & Shahino Mah Abdullah¹

¹Faculty of Science and Technology, Universiti Sains Islam Malaysia, Bandar Baru Nilai, 71800 Nilai, Negeri Sembilan, Malaysia

²Ionic Materials and Energy Devices Laboratory, Physics Department, Faculty of Science, Universiti Putra Malaysia, 43400 UPM, Serdang, Selangor Darul Ehsan, Malaysia

³Low Dimensional Material Research Centre (LDMRC), Department of Physics, Faculty of Science, University of Malaya, Kuala Lumpur 50603, Malaysia

Abstract

Fossil fuels contribute to air pollution and drive climate change. Transitioning to solar energy offers a cleaner alternative. Perovskite solar cells are a promising advancement, potentially exceeding silicon cell efficiencies with simpler, cost-effective manufacturing. This research demonstrates the feasibility of electricity generation using a solution-processed perovskite solar cell under low light in the room building. The fabricated cell achieved an open-circuit voltage of 1.49V and a short-circuit current density of 5.15 mA/cm². A maximum power conversion efficiency of 18.67% was obtained under only around 10% of actual one sun light intensity. Such a high obtained efficiency of solar cell fabricated using inexpensive materials under low light intensity has become our current work novelty. These results highlight the potential of cost-effective perovskite solar cells for indoor and ambient light energy harvesting, supporting a shift towards sustainable energy solutions.

Keywords : air pollution; solar cells; perovskite; efficiencies; ambient light

1.0 Introduction

The increasing reliance on fossil fuels for power generation has brought about significant environmental, health, and social concerns, necessitating cleaner and more sustainable energy sources. Burning fossil fuels causes global climate change, air and water pollution, land degradation, and disease, as emphasized by several studies [1,2,3]. The Intergovernmental Panel on Climate Change (IPCC) has emphasized the importance of the immediate reduction in greenhouse gas emissions to reverse the impacts of climate change [4]. Further, the hazardous chemicals released from fossil fuel-powered power plants, such as sulfur dioxide (SO₂) and nitrogen oxides (NO_x), are dangerous health risks, particularly for sensitive populations [5]. The limited supply of fossil fuels also raises concerns of resource depletion and environmental degradation, and therefore the need for alternative sources of energy [6].

Solar energy offers a strong alternative with a clean, renewable source of power and the ability to reduce greenhouse gas emissions significantly and improve air quality [7]. Compared to traditional fossil fuel power generation, solar power systems have no toxic emissions during operation and require minimal water use, thereby decongesting water resources [8]. The flexibility of solar energy systems facilitates installation on various types of land, minimizing habitat loss and land degradation. Solar power has the capability to create economic benefits and enhance energy security, particularly in regions with high solar radiation [9].

Even though there are advantages of solar energy, traditional silicon solar cells are highly effective outdoor and not indoors. This is a serious limitation in harnessing solar energy in urban areas where natural light is typically lacking. In response to this challenge, the objective of this study is to demonstrate the feasibility of generating electricity with a cost-effective solution-processed perovskite solar cell under illumination by room building light. This work stands out for its originality in using solution-processed perovskite solar cells for low-

light applications. The key materials applied in this work include a perovskite precursor and nickel (II) phthalocyanine-tetrasulfonic acid tetrasodium salt (NiTsPc), which would enhance energy conversion efficiency under low light conditions. The incorporation of NiTsPc as a sensitizer enhances light absorption, making the cells innovative and highly applicable for indoor environments.

The emergence of perovskite materials in solar cells technology is a great milestone in the quest for efficient and affordable renewable energy sources [10]. The ability of perovskite solar cells, processed through solution processing techniques, to be very promising in high power conversion efficiencies has been of great interest [11]. The present study revolves around increasing the efficiency, stability, and scalability of perovskite solar cells, with emerging technologies such as tandem solar cells and flexible substrates unlocking diverse applications [12,13]. With scientists exploring non-toxic and abundant materials for perovskite fabrication, the potential for clean solar energy solutions rises [14]. The work hopes to advance this emerging research field by exploring the performance of perovskite solar cells in indoor illumination, hence opening the potential application areas of solar energy technology for cities. These cells can power IoT devices, sensors, and other low-energy electronics, offering a sustainable alternative to batteries.

2.0 Materials

2.1 Fluorine-doped tin oxide (FTO) glass

In the current study, a perovskite solar cell was fabricated with a highly selected set of materials, with each material assigned a specific function in enhancing the general efficiency of the solar cell. The most dominant substrate material used in the production of the solar cell is fluorine-doped tin oxide (FTO) glass. This material is specifically utilized as a highly conducting and transparent substrate, allowing light through while ensuring proper electrical conductivity [15]. The FTO serves a vital function in allowing the electrons from the photoactive layers to be moved to the outside circuit, thus ensuring efficient energy conversion.

2.2 Titanium dioxide (TiO_2)

The second critical component is titanium dioxide (TiO_2), which serves as the electron transport layer in the solar cell device. TiO_2 is described as a wide bandgap semiconductor that is noted for its efficient uptake of ultraviolet light and for its ability to promote the transport of electrons that are generated from the dye upon light absorption [16]. TiO_2 is normally used in porous film form, thus providing a large surface area that is favorable for the adsorption of the sensitizing dye, NiTsPc. This structure greatly enhances the overall efficiency of the solar cell by maximizing the interaction between the semiconductor and the dye.

2.3 Nickel (II) phthalocyanine-tetrasulfonic acid tetrasodium salt (NiTsPc)

The light absorption material in this solar cell fabricated is nickel (II) phthalocyanine-tetrasulfonic acid tetrasodium salt (NiTsPc). The blue dye is pivotal in light absorption, thus allowing the production of excited electrons when the solar cell is illuminated by visible light. The excited electrons then travel through the TiO_2 film, hence initiating the charge separation. The absorption spectrum for NiTsPc exhibits a very strong resemblance with the solar spectrum, thus allowing efficient light harvesting and energy conversion that is vital in ensuring maximum solar cell efficiency [17].

2.4 Iodine

Iodine is incorporated in the operating mechanism in the form of a redox mediator in the electrolyte medium. The major function is the regeneration process after the dye has been injected with electrons in the TiO_2 film. The iodine species, in particular in the I_3^- form, serve as charge transporters in the cell, ensuring the continuity of the electronic current and enhancing the solar cell efficiency in the process [18]. Regenerative process is essential for the extended use of the solar cell.

2.4 Perovskite precursor ink

The perovskite precursor ink that was applied in the current study was purchased from Ossila and is specially designed for processing in ambient condition. The perovskite ink is made from a combination

of methyl ammonium iodide (MAI) and lead chloride (PbCl_2) dissolved in dimethyl formamide (DMF). When heated, this ink is converted to a methylammonium lead halide perovskite, eventually forming

methylammonium lead iodide with little chlorine, with the chemical formula $\text{CH}_3\text{NH}_3\text{PbI}_{3-x}\text{Cl}_x$. This perovskite material is commonly used in the construction and design of solar cells and can be utilized in both standard and inverted configurations [19]. The ink exhibits the ability to attain power conversion efficiency (PCE) values that surpass 13%, making it a very important material in thin film organic solar cell production.

2.5 Carbon conductive paste

Aside from the above-stated function, conductive carbon paste is also utilized as a counter electrode in solar cell design [20]. The material provides a conductive interface that favors the extraction of electrons from the outside circuit. The addition of carbon paste helps greatly in charge collection efficiency and is also vital in ensuring the stability and durability of the solar cell. Carbon paste ensures the efficient operation of the solar cell by limiting resistive losses, thus making it a vital component in the overall design.

3.0 Methodology

The production process of the perovskite solar cell commences with the precise measurement of 1.5 grams of titanium dioxide (TiO_2), which serves as the electron transport layer in the solar cell. To prepare an appropriate paste for application, TiO_2 is combined with 1 ml of polyethylene glycol (PEG) and 1 ml of ethanol with 99.99 in a ceramic vessel. The inclusion of PEG functions as a binder, enhancing the adhesion of TiO_2 particles to the substrate while also providing mechanical stability to the film. Ethanol is incorporated as a solvent to dissolve the TiO_2 and PEG mixture, resulting in a uniform consistency that is ready for direct application onto the substrate.

Upon complete dissolution of the mixture through extensive agitation, the resulting solution is then deposited onto the conducting surface of fluorine-doped tin oxide (FTO) glass by means of doctor blade technique. This process enables a controlled and uniform deposition of the TiO_2 mixture over about half of the FTO glass surface area. The coated FTO glass (Fig. 1) is subsequently heated at a temperature of 200°C by using hot plate for a period of 10 minutes in order to enhance the formation of a strong TiO_2 layer while removing solvent residue. After thermal treatment, the glass is allowed to cool down to room temperature, which in effect solidifies the TiO_2 layer and readies it for further processing.

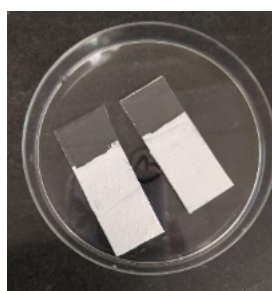


Fig. 1: TiO_2 particles coated on FTO glass.

The dye solution was prepared by mixing 1 ml of deionized (D.I) water and 10 mg of nickel (II) phthalocyanine-tetrasulfonic acid tetrasodium salt (NiTsPc). In this process, the dye serves as a sensitizer in the solar cell, while the use of D.I. water ensures removal of any contaminants that may interfere with the solar cell's efficiency. The pre-coated fluorine-doped tin oxide (FTO) glass, which has been pre-coated with titanium dioxide (TiO_2), is treated with the mixture of NiTsPc and D.I. water for a longer period, that is, overnight. The longer immersion in the solution enhances maximum

adsorption of the dye onto the surface of the TiO_2 (Fig. 2), thus maximizing the light-absorbing properties, as well as the overall solar cell efficiency.

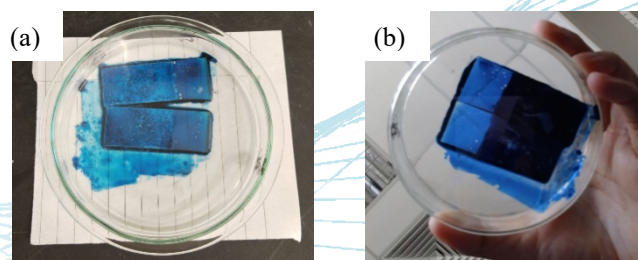


Fig. 2: (a) FTO coated glass with TiO_2 layer immersed in NiTsPc overnight; (b) bottom view of the substrate with TiO_2 and NiTsPc.

After long immersion, the FTO glass is removed from the solution, and the uncoated areas of the glass are carefully purified in order to remove any possible hindrance from the operational effectiveness of the solar cell. The glass is then annealed at $90^\circ C$ for 20 minutes (Fig. 3) until it is fully dry, allowing the dye to adhere onto the TiO_2 layer.



Fig. 3: Annealing process of the coated FTO glass at $90^\circ C$.

In preparation for the counter electrode, another clean piece of FTO glass is applied with carbon paste to its conductive surface, covering about half of the area (2.5×2.0 cm). This carbon paste serves as the conductive layer that will facilitate electron collection. The FTO glass with carbon paste is then heated at $100^\circ C$ for 10 minutes until dry (Fig. 4), ensuring a solid and conductive layer.

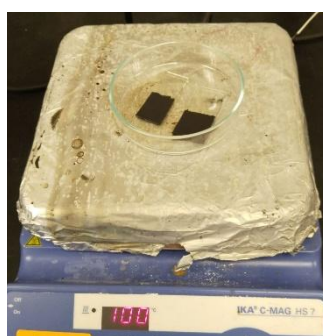


Fig. 4: The FTO glass with carbon paste is then heated at $100^\circ C$.

After the successful preparation of the electrode, $1.6\mu l$ iodine are carefully deposited onto the TiO_2 surface by using micropipette. The purpose of this iodine is that it acts as a redox mediator in the

solar cell, allowing for the regeneration of the dye after it has been injected with electrons in the TiO_2 film. $0.8\mu l$ of perovskite solution was then deposited onto the same TiO_2 surface using micropipette, thus allowing the iodine and perovskite interaction that forms a functional charge-separation enhancing layer.

The final phase of the assembly process involves the attachment of the carbon paste-treated FTO glass onto the surfaces of TiO_2 , iodine, and perovskite such that the latter layers face each other (Fig. 5). This particular positioning enables efficient charge transfer between the layers. To analyze the functional efficacy of the perovskite solar cell, the assembled device is connected to a source-measure unit, which tests both the efficiency and general function of the solar cell under low light intensity of about $10\text{-}12\text{ mW/cm}^2$ (input power, P_{in}) to imitate indoor light range or ambient light conditions. This systematic approach ensures that all elements in the perovskite solar cell are carefully crafted and optimized for maximum efficiency, leading to a holistic improvement in the device.

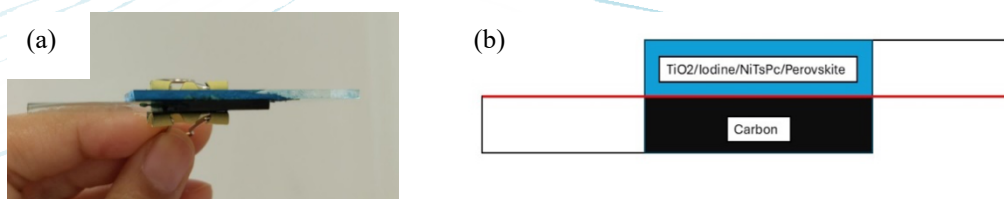


Fig. 5: (a) the attachment of surfaces of TiO_2 , iodine, and perovskite onto carbon paste-coated FTO glass; (b) drawing of the layer structure.

4.0 Results and Discussion

Fig. 6 shows the current density (J_{sc}) against a voltage (V) curve. From this curve, the two main parameters can be directly extracted: the short-circuit current density (J_{sc}), defined as the current density at 0 V, and the open-circuit voltage (V_{oc}), defined as the voltage at 0 current density. Maximum J_{sc} is found to be 5.15 mA/cm^2 , while maximum V_{oc} is 1.49 V. Besides, the general appearance of this curve gives a qualitative idea of the fill factor (FF) that describes how efficiently the cell delivers maximum power. A more rectangular shape corresponds to a bigger FF, while the observed linear slope correlates to a lower FF, which, according to the FF formula (Eq. 1), amounts to 0.29. The lower value (< 0.80) implies that the cell is not working at the maximum efficient state due to internal resistances and other losses [21].

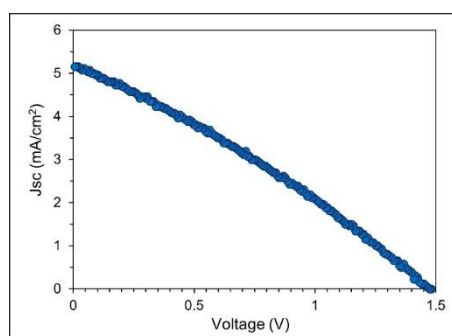


Fig. 6: Current density (J_{sc}) versus voltage (V).

$$FF = \frac{J_{max} \times V_{max}}{J_{sc} \times V_{oc}} \quad (1)$$

To quantify the solar cell's performance, we calculate the power conversion efficiency (PCE), which is given by Eq. 2:

$$PCE = \frac{V_{oc} \times J_{sc} \times FF}{P_{in}} \times 100 \quad (2)$$

Where V_{oc} is the open-circuit voltage, J_{sc} is the short circuit current density, FF is the fill factor, and P_{in} is the incident solar power (mW/cm^2).

Fig. 7 presents the power density versus voltage curve derived from Fig. 7. To calculate the power at a specific point on the J-V curve, one multiplies the current density and voltage values. Subsequently, this power value is plotted against the corresponding voltage to generate the power curve. The maximum power point (MPP), which represents the highest electrical power output from the cell, corresponds to the peak of this curve. The voltage at this peak is defined as the maximum power point voltage (V_{max}), while the power value at this peak is designated as the maximum power (P_{max}). In this case, V_{max} is 0.8 V, and the power output reaches approximately $2.25 \text{ mW}/\text{cm}^2$. The power curve visually demonstrates how the power output from the solar cell varies with voltage, emphasizing the significance of operating the solar cell at the MPP to achieve optimal performance.

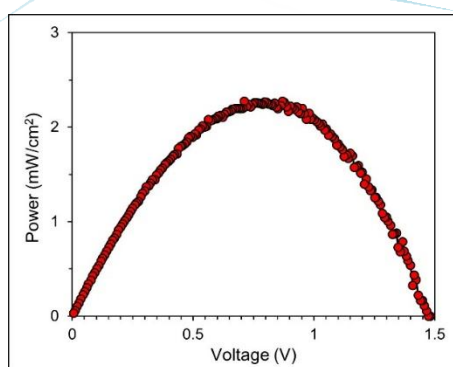


Fig. 7: Power density (P) versus voltage (V).

The analyzed perovskite solar cell has a power conversion efficiency of 18.67% after considering low light intensity applied on the cell ($10 - 12 \text{ mW}/\text{cm}^2$, instead of $100 \text{ mW}/\text{cm}^2$ or 1 Sun). This efficiency, however, does provide evidence of its capacity to convert light into electricity [22]. The efficiency of a perovskite cell is very much dependent on the specific perovskite materials, the fabrication methods, and the environmental conditions under which it is tested. Some of the important parameters for evaluation of the cell performance are undeniably the short-circuit current density (J_{sc}) of $5.15 \text{ mA}/\text{cm}^2$ and an open-circuit voltage (V_{oc}) of 1.49 V. A high V_{oc} values indicate that the device is well capable of allowing charge separations, thus it is able to generate a relatively high potential difference. Its J_{sc} value is an indication of its ability to produce current in case no external resistance applies.

However, a critical aspect of this cell's performance lies in its fill factor (FF), which is 0.29. The fill factor is a measure of the "squareness" of the current-voltage (I-V) curve and is indicative of the efficiency with which the cell can deliver power. A low fill factor (FF), as observed in this study, indicates that the cell's I-V curve deviates significantly from the ideal rectangular shape, suggesting the presence of losses within the device. Several factors can contribute to a low FF. High series resistance within the cell can hinder current flow, while low shunt resistance may result in current leakage, both of which lead to a diminished FF [23]. Additionally, recombination losses, where charge carriers recombine before contributing to the current, can further impact the fill factor. Issues at the interfaces between the various layers of the perovskite cell structure can also negatively affect the FF. The I-V curve presented in the data visually supports the observation of a low FF, exhibiting a relatively linear slope instead of the sharp "knee" and rectangular shape characteristic of an ideal cell.

The Power-Voltage curve is a crucial tool in understanding the maximum power point (MPP) of a solar cell. It shows how the power output varies with the voltage across the cell, emphasizing the importance of operating the cell at the MPP for maximum performance. The I-V curve, with a general linear trend, provides insights into non-idealities of the cell. It shows that the slope of the I-V curve correlates to the cell's resistance, with higher slopes implying lower resistance. To increase the low fill factor in a perovskite cell, improvements in conductivity, shunt resistance, and recombination losses are needed. Additionally, optimizing interfaces between cell layers is also necessary.

5.0 Conclusion

This research has successfully demonstrates the capability of generating energy from a solution-processed perovskite solar cell under ambient light circumstances. The device showed promising performance, with an open-circuit voltage of 1.49 V and a short-circuit current density of 5.15 mA/cm². Furthermore, a power conversion efficiency of 18.67% was achieved after considering low light intensity applied on the cell (10 - 12 mW/cm²) which is only approximately 10% of actual 1 Sun light intensity. These findings indicate that solution-processed perovskite solar cells may generate electricity under ambient illumination, indicating their potential for use in indoor energy harvesting and contributing to the development of sustainable energy solutions. While additional optimisation is required, the findings provide a solid foundation for the usage of perovskite solar cells in low-light situations, broadening their application beyond traditional outdoor solar energy generation.

Acknowledgements

This research was supported by Universiti Sains Islam Malaysia under USIM Research Grant (PPPI/USIM/FST/USIM/112623). The research was also funded by the Ministry of Higher Education, Malaysia under the Fundamental Research Grant Scheme (FRGS/1/2024/STG07/USIM/02/1).

References

- [1] N. Watts et al. (2021). The 2020 report of The Lancet Countdown on health and climate change: responding to converging crises. *The Lancet*, vol. 397, no. 10269, pp. 129–170, doi: 10.1016/S0140-6736(20)32290-X/ASSET/5FD758AB-B9B7-42F2-B3DB-9C112BB19C89/MAIN.ASSETS/GR15_LRG.JPG
- [2] A. Hassan, S. Z. Ilyas, A. Jalil, and Z. Ullah. (2021). Monetization of the environmental damage caused by fossil fuels. *Environmental Science and Pollution Research*, vol. 28, no. 17, pp. 21204–21211, doi: 10.1007/S11356-020-12205-W/FIGURES/1
- [3] A. Bhatnagar. (2022). Cardiovascular Effects of Particulate Air Pollution. *Annu Rev Med*, vol. 73, no. Volume 73, pp. 393–406, doi: 10.1146/ANNUREV-MED-042220-011549/CITE/REFWORKS
- [4] A. Monteiro, J. Ankrah, H. Madureira, and M. O. Pacheco. (2022). Climate Risk Mitigation and Adaptation Concerns in Urban Areas: A Systematic Review of the Impact of IPCC Assessment Reports. *Climate*, vol. 10, no. 8, p. 115, doi: 10.3390/CLH10080115/S1
- [5] R. K. Karduri and C. Ananth. (2023). Transitioning rural communities to renewable energy: Challenges and successes. *SSRN Electronic Journal*, vol. 8, no. 5, doi: 10.2139/ssrn.4637835
- [6] M. T. Kartal, S. Kılıç Depren, F. Ayhan, and Ö. Depren. (2022). Impact of renewable and fossil fuel energy consumption on environmental degradation: evidence from USA by nonlinear approaches. *International Journal of Sustainable Development and World Ecology*, vol. 29, no. 8, pp. 738–755, doi: 10.1080/13504509.2022.2087115.
- [7] A. O. M. Maka and J. M. Alabid. (2022). Solar energy technology and its roles in sustainable development. *Clean Energy*, vol. 6, no. 3, pp. 476–483, doi: 10.1093/CE/ZKAC023
- [8] U. Mehmood. (2021). Contribution of renewable energy towards environmental quality: The role of education to achieve sustainable development goals in G11 countries. *Renewable Energy*, vol. 178, pp. 600–607, doi: 10.1016/J.RENENE.2021.06.118
- [9] J. Zhao et al. (2022). The determinants of renewable energy sources for the fueling of green and sustainable economy. *Energy*, vol. 238, p. 122029, doi: 10.1016/J.ENERGY.2021.122029
- [10] P. Yan, D. Yang, H. Wang, S. Yang, and Z. Ge. (2022). Recent advances in dopant-free organic hole-transporting materials for efficient, stable and low-cost perovskite solar cells. *Energy Environ Sci*, vol.

15, no. 9, pp. 3630–3669, doi: 10.1039/D2EE01256A

- [11] D. K. Lee and N. G. Park. (2022). Materials and Methods for High-Efficiency Perovskite Solar Modules. *Solar RRL*, vol. 6, no. 3, p. 2100455, doi: 10.1002/SOLR.202100455
- [12] P. Zhang, M. Li, and W. C. Chen. (2022). A Perspective on Perovskite Solar Cells: Emergence, Progress, and Commercialization. *Front Chem*, vol. 10, p. 802890, doi: 10.3389/FCHEM.2022.802890/BIBTEX
- [13] A. W. Y. Ho-Baillie, J. Zheng, M. A. Mahmud, F. J. Ma, D. R. McKenzie, and M. A. Green. (2021). Recent progress and future prospects of perovskite tandem solar cells. *Appl Phys Rev*, vol. 8, no. 4, doi: 10.1063/5.0061483/979963
- [14] M. F. García-Mendoza et al. (2023). CaTiO₃ perovskite synthesized by chemical route at low temperatures for application as a photocatalyst for the degradation of methylene blue. *Journal of Materials Science: Materials in Electronics*, vol. 34, no. 10, pp. 1–11, doi: 10.1007/S10854-023-10309-W/FIGURES/13.
- [15] K. Gossen and A. Ehrmann. (2020). Influence of FTO glass cleaning on DSSC performance. *Optik (Stuttg)*, vol. 183, pp. 253–256, doi: 10.1016/J.IJLEO.2019.02.041
- [16] W. Hu, S. Yang, and S. Yang. (2020). Surface Modification of TiO₂ for Perovskite Solar Cells. *Trends Chem*, vol. 2, no. 2, pp. 148–162, doi: 10.1016/J.TRECHM.2019.11.002
- [17] A. Kolay, P. Ghosal, and M. Deepa. (2020). Novel Integration of Nickel Phthalocyanine/Nickel Oxide-Based Photocathodes and Copper-Encapsulated Carbon-Dot-Cosensitized Photoanodes in Tandem for a Highly Efficient Solar Cell. *ACS Sustain Chem Eng*, vol. 8, no. 23, pp. 8593–8603, doi: 10.1021/ACSSUSCHEMENG.0C01107/SUPPL_FILE/SC0C01107_SI_001.PDF
- [18] H. Yang et al. (2023). Enhancing the Stability of Perovskite Solar Cells through an Iodine Confining Strategy. *ACS Energy Lett*, vol. 8, no. 9, pp. 3793–3799, doi: 10.1021/ACSENERGYLETT.3C01330/SUPPL_FILE/NZ3C01330_SI_001.PDF
- [19] E. Berger et al. (2022). Recent developments in perovskite-based precursor inks for scalable architectures of perovskite solar cell technology. *Sustain Energy Fuels*, vol. 6, no. 12, pp. 2879–2900, doi: 10.1039/D2SE00162D
- [20] M. Wu, M. Sun, H. Zhou, J. Y. Ma, and T. Ma. (2020). Carbon Counter Electrodes in Dye-Sensitized and Perovskite Solar Cells. *Adv Funct Mater*, vol. 30, no. 7, p. 1906451, doi: 10.1002/ADFM.201906451.
- [21] A. Bouzaher, A. Terki, and M. T. Bouzaher. (2023). Photovoltaic Panel Faults Diagnosis: Based on the Fill Factor Analysis and Use of Artificial Intelligence Techniques. *Arab J Sci Eng*, vol. 48, no. 5, pp. 6471–6487, doi: 10.1007/S13369-022-07409-W/TABLES/8.
- [22] S. Khatoun et al. (2023). Perovskite solar cell's efficiency, stability and scalability: A review. *Mater Sci Energy Technol*, vol. 6, pp. 437–459, doi: 10.1016/J.MSET.2023.04.007.
- [23] G. D. Obikoya, A. Soman, U. K. Das, and S. S. Hegedus. (2023). Investigation into fill factor and open-circuit voltage degradations in silicon heterojunction solar cells under accelerated life testing at elevated temperatures. *Solar Energy Materials and Solar Cells*, vol. 263, p. 112586, doi: 10.1016/J.SOLMAT.2023.112586